SANDIA REPORT
SAND2012-8103
Unlimited Release
Printed Month and Year

Doped Solid Oxide Fuel Cell Electrolytes Produced via Combination of Suspension Plasma Spray and Very Low Pressure Plasma Spray

James Dean Fleetwood, Prof. Elliott Slamovich, Prof. Rodney Trice, Aaron C. Hall, James McCloskey

Prepared by
Sandia National Laboratories
Albuquerque, New Mexico 87185 and Livermore, California 94550

Sandia National Laboratories is a multi-program laboratory managed and operated by Sandia Corporation, a wholly owned subsidiary of Lockheed Martin Corporation, for the U.S. Department of Energy's National Nuclear Security Administration under contract DE-AC04-94AL85000.

Approved for public release; further dissemination unlimited.

Sandia National Laboratories

Issued by Sandia National Laboratories, operated for the United States Department of Energy by Sandia Corporation.

NOTICE: This report was prepared as an account of work sponsored by an agency of the United States Government. Neither the United States Government, nor any agency thereof, nor any of their employees, nor any of their contractors, subcontractors, or their employees, make any warranty, express or implied, or assume any legal liability or responsibility for the accuracy, completeness, or usefulness of any information, apparatus, product, or process disclosed, or represent that its use would not infringe privately owned rights. Reference herein to any specific commercial product, process, or service by trade name, trademark, manufacturer, or otherwise, does not necessarily constitute or imply its endorsement, recommendation, or favoring by the United States Government, any agency thereof, or any of their contractors or subcontractors. The views and opinions expressed herein do not necessarily state or reflect those of the United States Government, any agency thereof, or any of their contractors.

Printed in the United States of America. This report has been reproduced directly from the best available copy.

Available to DOE and DOE contractors from
U.S. Department of Energy
Office of Scientific and Technical Information
P.O. Box 62
Oak Ridge, TN 37831

Telephone: (865) 576-8401
Facsimile: (865) 576-5728
E-Mail: reports@adonis.osti.gov
Online ordering: http://www.osti.gov/bridge

Available to the public from
U.S. Department of Commerce
National Technical Information Service
5285 Port Royal Rd.
Springfield, VA 22161

Telephone: (800) 553-6847
Facsimile: (703) 605-6900
E-Mail: orders@ntis.fedworld.gov
Online order: http://www.ntis.gov/help/ordermethods.asp?loc=7-4-0#online

SAND2012-8103achal
Unlimited Release
Printed October 2012

Doped Solid Oxide Fuel Cell Electrolytes Produced via Combination of Suspension Plasma Spray and Very Low Pressure Plasma Spray

James D. Fleetwood, Prof. Elliott Slamovich, Prof. Rodney Trice
Department of Materials Science and Engineering
Purdue University
701 Stadium Avenue
West Lafayette, IN 47907

Aaron C. Hall, James McCloskey
Coatings and Surface Engineering, 01832
Sandia National Laboratories
P.O. Box 5800, MS1130
Albuquerque, New Mexico 87185-1130

Abstract

Solid oxide fuel cells (SOFCs) are a promising element of comprehensive energy portfolio due to their direct mechanism for converting the oxidization of fuel, such as hydrogen, into electrical energy. Plasma spray allows deposition of high melting temperature SOFC feedstock on complex surfaces, such as in non-planar SOFC designs. Dense, thin electrolytes of ideal composition for SOFCs can be created by suspension plasma spraying in a very low pressure environment. Compositional control is achieved with dissolved dopant compounds that are incorporated into the coating during spraying. In the work reported, sub-micron 8 mole% Y_2O_3-ZrO_2 (YSZ) powders, in suspension with scandium-nitrate dopants, were sprayed on NiO-YSZ anodes, at Sandia National Laboratories' Thermal Spray Research Laboratory. The spray chamber was held at 2.4-10 Torr, with the plasma composed of argon, hydrogen, and helium. The resultant electrolytes were 2-10 microns thick. Electrolyte microstructure and performance as part of a SOFC system is reported.

ACKNOWLEDGMENTS

The author would like to thank Dr. Patricia Metcalf of Purdue University for her help with laboratory equipment, as well as Francoise Anguoa and Kent VanEvery for their work on SOFC testing and suspension plasma spray, respectively. James McCloskey, Dr. Aaron Hall, Marlene Knight, and Dave Urrea were all very helpful at the Thermal Spray Research Laboratory. Finally, the advice of Prof. Rodney Trice, Prof. Elliott Slamovich, and Dr. Aaron Hall in deciding the direction of this research was most valuable.

CONTENTS

1. Introduction 9
   1.1. Solid Oxide Fuel Cells (SOFCs) 10
   1.2. Very Low Pressure Plasma Spray (VLPPS) 11
   1.3. Suspension Plasma Spray (SPS) 12

2. Experimental Procedure 13
   2.1. Suspension Preparation 13
   2.2. Substrate Preparation 14
   2.3. Substrate Holders 15
   2.4. Coating Creation at the Thermal Spray Research Laboratory 16
   2.5. SOFC Testing at Purdue University 20

3. Results & Discussion 21
   3.1. Scanning Electron Microscopy (SEM) 21
   3.2. X-Ray Diffraction (XRD) 28
   3.3. Fuel Cell Performance 28

4. Conclusions 31
   4.1. List of Publications, Presentations, Awards, etc. 32

5. References 33

Distribution [can go on an even or an odd page] 35

FIGURES

Figure 1 Basic diagram of SOFC function [2]. 11
Figure 2. Coulter Counter measurement of particle size for 8 mole % YSZ from Inframat Advanced Materials. 13
Figure 3. Overview of suspension preparation 14
Figure 4. Images of the die (left) used to laminate the anode layers as seen on the right image showing the progression: (a) unlaminated sheets of NiO-YSZ, (b) hot-pressed laminated sheets of NiO-YSZ, (c) sintered laminated sheets of NiO-YSZ (in oxidized state), (d) sintered laminated sheets of NiO-YSZ (in reduced state), (e) an example of the initial material system used: NiO-YSZ with a YSZ electrolyte laminated sheet on top, (f) a sintered version of (e), in which the electrolyte delaminated, and (g) a complete fuel cell after testing, showing the cathode side (the white border is the bonding cement, the dark grey is the LSM-YSZ cathode material with platinum electrodes bonded to it, and the pearlescent area is exposed electrolyte) 15
Figure 5. Image of the stair step sample holder, with substrates loaded. 15
Figure 6. Image of the cold plate sample holder. This sample holder allowed for a reduction in substrate temperature and an increase in temperature stability over the course of a spray run. 16
Figure 7. Image of the vacuum chamber at the TSRL. 16
Figure 8. Diagram of the cathode and anode setup used at the TSRL. 17

Figure 9. A diagram of a complete SOFC with electrodes attached using a four point method. A side view can be seen in the above image, while a top view/bottom view can be seen in the lower image. 20
Figure 10. An image of the fuel cell testing rig outside of the furnace and fume hood, showing: (a) the cathode-side of the SOFC, (b) the cathode-side platinum electrode wires that attach to the fuel cell, (c) the cathode-side platinum wire measurement output connections, (d) the H_2 gas input tube, (e) the exhaust gas tube (which feeds through two bubblers and out a fume hood), and (f) the anode-side platinum wire measurement output connections. 20
Figure 11: SEM images of the initial microstructures of select SPS/VLPPS coatings. On left is a cross-section of an un-doped 1 vol.% YSZ coating sprayed for 10 minutes at 46" standoff. On right is a surface image of a 3 mol% Sc-doped 0.5 vol.% YSZ coating sprayed for 7 minutes at 43". Note the presence of unmelted particles in the cross-section image, despite significant density of the coating, and the surface roughness of the right image. 22
Figure 12: SEM image of a complete fuel cell after testing. The spray conditions were 8 mol% Sc-doped 0.5 vol% YSZ, sprayed for 7 min at 49". Note that in the fuel cell preparation, the coating undergoes a 1200º C - 2 hour heat treatment, which causes some sintering and the subsequent disappearance of clear remnant particles in the coating, as seen in Figure 11..... 22
Figure 13: SEM images of 0.5 vol% YSZ, sprayed for 7 min at 43" (left) and 49" (right). While this comparison would suggest a moderate increase in thickness for the closer standoff distance, this is attributed to the surface roughness induced variability in coating thickness associated with comparing any two individual sections of coatings. See Figure 14 and Figure 15 for further evidence of this. 23
Figure 14: SEM images of 8 mol. % Sc-doped 0.5 vol% YSZ, sprayed for 7 min at 43" (left) and 49" (right). This comparison suggests a slight increase in coating thickness caused by increasing standoff distance within this 6" range. However, as seen in Figure 13, this is a byproduct of the bias associated with comparing any two small sections of coatings. See Figure 15 for further evidence of this. 24
Figure 15: SEM images at higher magnification of the same coatings from Figure 13, 8 mol. % Sc-doped 0.5 vol% YSZ, sprayed for 7 min at 43" (left) and 49" (right). This comparison suggests there is no effect on coating thickness caused by changing standoff distance within this 6" range. See Figure 13 and Figure 14 for further evidence of this. 25
Figure 16: SEM images of 0.25 vol.% YSZ (left) and 1 vol.% YSZ (right), sprayed for 10 min at 43" (left) and 49" (right). As expected, this comparison shows a distinct increase in coating thickness associated with increased powder loading. 26
Figure 17: SEM images of 0.5 vol% YSZ, sprayed for 7 min at 43" with doping of 3 mol% Sc (left) and 8 mol% Sc (right). The microstructures are too similar to mark a definitive difference between the doping levels, though initial fuel cell testing has shown increasing performance with doping. 27
Figure 18: SEM image and EDS map of a complete fuel cell with an electrolyte created with 8 mol% Sc-doped 0.5 vol% YSZ, sprayed for 7 min at 49". The EDS map clearly shows the presence of scandium (blue) in the electrolyte. 27
Figure 19: XRD spectrum comparison between undoped, 1.5 mol% Sc_2O_3, and 4 mol% Sc_2O_3 electrolyte coatings prepared on a NiO-YSZ substrate. No peaks were associated with a separate Sc_2O_3 phase. 28

Figure 20: Potentiodynamic testing results comparing an 8 mol% Sc doped 0.5 vol% YSZ, sprayed for 7 min at 49" to a standard cell, made from similar components, including a YSZ electrolyte, purchased from Fuel Cell Materials, Inc. 29

TABLES

Table 1. Measurements taken by Dorier et al 800 mm down the axis from the nozzle of a Sulzer Metco 03CP spray gun operated at 1500 A and 43 V, with plasma formed of H_2/Ar at 3/100 SLPM [6]. 12
Table 2. Operating parameters for samples created in May 2010 visit to TSRL..... 17
Table 3. Operating parameters for samples created in summer 2011 visit to TSRL. 18
Table 4. Operating parameters for samples created in March 2012 visit to TSRL. 19

NOMENCLATURE

CAPS	Controlled Atmosphere Plasma Spray
DOE	Department of Energy
EDS	Energy Dispersive Spectroscopy
NASA	National Aeronautics and Space Administration
NiO	Nickel Oxide
$Sc(NO_3)_3XH_2O$	Scandium Nitrate
SEM	Scanning Electron Microscopy
SOFC	Solid Oxide Fuel Cell
SPS	Suspension Plasma Spray
SNL	Sandia National Laboratories
TSRL	Thermal Spray Research Laboratory
VLPPS	Very Low Pressure Plasma Spray
XRD	X-ray Diffraction
YSZ	Yttria Stabilized Zirconia

1. INTRODUCTION

Worldwide energy problems are alarming because there is an ongoing rise in demand for energy coupled with simultaneous and continued depletion of energy resources. The solution to our energy crisis will require every available energy technology, including nuclear, solar, wind, clean-burning coal, and hydrogen. Solid oxide fuel cells (SOFCs), which can be powered by hydrogen, are a promising part of the solution because they provide a direct mechanism for converting the oxidization of fuel into electrical energy. They have a relatively simple design, conducive to durability and longevity. Essentially, oxygen in the form of air is supplied to a cathode where O^{2-} is formed, which diffuses through an oxygen conducting electrolyte to the anode. Fuel, in the form of hydrogen is supplied to the anode where hydrogen reacts with O^{2-} to form H_2O, releasing electrons to complete the circuit. Advantages of SOFCs include increased efficiency, no moving parts of traditional competing technologies, no expensive platinum catalysts, and decreased emission of SO_x and NO_x.

Despite success developing SOFCs in the past 15+ years, there is still need for improvement of current SOFC technology, particularly electrolyte materials. The ideal electrolyte is: (1) applied easily to non-planar shapes to take advantages of tubular SOFC designs, (2) both dense and thin (<50 μm), and (3) has optimized oxygen ion conductivity. Plasma spray coating techniques are a very promising way to prepare electrolytes on complex surfaces, thus satisfying criterion 1. However, conventional plasma-deposited coatings have high porosities and cannot be applied in thin layers (<50 μm) suitable for electrolytes. Also, control of the electrolyte composition is limited to the composition of the plasma spray feed stock powders.

A solution to forming thin, dense electrolytes of ideal composition for SOFCs is possible by combining suspension plasma spray (SPS), a new spray technique being developed by Purdue Prof. Rodney Trice, with some unique plasma spray equipment available at Sandia National Laboratories' (SNL) Thermal Spray Research Laboratory (TSRL). SPS feeds a suspension of very small powders within a solvent into the plasma. The solvent is evaporated, and the powders are melted and propelled toward a substrate. Stacking of the melted powders forms the coating (i.e. the electrolyte for this application). Prof. Trice brought this technique to Sandia National Laboratories as part of a faculty sabbatical and has used it to spray thin (<10 micron), dense coatings using the very low pressure plasma spray system (VLPPS) at TSRL.[1] Thus, criterion 2 for electrolytes was satisfied through a partnership between Purdue and SNL.

The need to optimize oxygen ion conductivity (criterion 3) can also be tailored using SPS. As stated previously, SPS involves making a suspension of nominally micron-sized powders in a solvent, then feeding it into a plasma. Prof. Trice has shown that

[1] Note that all SNL operating procedures and the pressure safety data package have been completed for this process.

other compounds dissolved in the suspension (i.e. dopants) are incorporated into the coating during plasma spraying. Thus, it is possible to change the chemistry of the micron-sized powder during the short millisecond time the powder/dopant is in the hot spray plume. This means that it is possible to quickly and systematically change the composition of the sprayed SOFC electrolyte to optimize its oxygen-ion conductivity by simply adjusting the suspension composition.

It is important to again note that while SPS makes it possible to easily adjust the composition of the final electrolyte, SPS combined with conventional air plasma spray does not produce the thin, dense electrolytes required for SOFCs. Whereas, the Very Low Pressure Plasma Spray (VLPPS) process, allows for the realization of all three criteria required for SOFC electrolytes. Initially, this process capability was only domestically available at Sandia's Thermal Spray Research Laboratory (TSRL), though this has recently expanded to include a facility at NASA Glenn Research Center as interest in the process has grown.

1.1. Solid Oxide Fuel Cells (SOFCs)

Solid oxide fuel cells (SOFCs) are a type of hydrogen fuel cell in which the anode, electrolyte, and cathode are composed of oxide ceramics. SOFCs can achieve efficiencies of 65%, with higher efficiencies available in cogeneration systems, such as when combined with turbine engines. A diagram of hydrogen fuel cell operation can be seen in Figure 1. During hydrogen fuel cell operation, O_2 is first reduced at the cathode. It then diffuses through the electrolyte and oxidizes the H_2 at the anode, creating H_2O. The electrolyte must be electrically insulating and impermeable, conducting only the oxygen ions. This separates the electrochemical reactions, forcing the electrons to travel in a circuit between the electrodes, allowing for power generation. The electrode materials are both electronically and ionically conductive, while also serving to catalyze H_2 oxidation at the anode and O_2 reduction at the cathode [1]. The Nernst equation, seen in Equation 1, describes the electrochemical potential between the cathode and anode, where R is the gas constant, 8.314 J/mol·K, F is Faradays' constant, 9.649×10^4 C/mol, T is temperature, and P_{O_2} is partial pressure of oxygen.

$$\boldsymbol{V = E = \frac{RT}{4F} \ln \left[\frac{P_{O_2}^{(cathode)}}{P_{O_2}^{(anode)}} \right]}$$

Equation 1

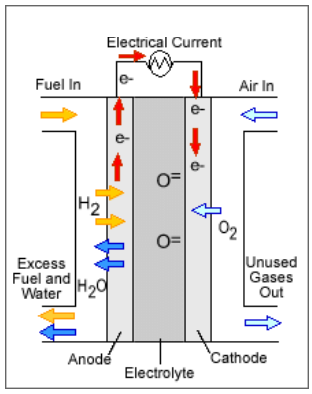

Figure 1 Basic diagram of SOFC function [2].

The ionic conductivity of oxygen is facilitated by the presence of oxygen vacancies, V_O^{**}, in the lattice and the mobility of these vacancies. Oxygen vacancies are created intrinsically via thermal excitation and extrinsically via charge compensation due to the displacement of the cation with dopant atoms of differing valence. The extrinsic doping effect in YSZ is represented in Equation 2, below.

$$Y_2O_3 \rightarrow 2Y_{Zr}^{'} + V_O^{**} + 3O_O^{x}$$

Equation 2

Doping is the source of the majority of V_O^{**}, though thermal excitation is still necessary to overcome the energy barrier for vacancy motion. This necessitates operating temperatures >600 °C, often 800-1000 °C [3].

In choosing dopant elements, the ionic radius is an important consideration after the valence necessary for vacancy creation. With elements of larger radius than zirconium, vacancies tend to coordinate with the zirconium. This leads towards stability of the tetragonal and cubic phases under lower dopant concentrations than with smaller radius elements. However, the highest energy barrier of the oxygen diffusion path is around the dopant and this energy barrier increases with ionic radius. These effects suggest that the ideal dopant is one with a radius equal to zirconium and failing that, one that is minimally larger [4]. Scandium, with an ionic radius of 88.5 pm to zirconium's 86 pm is the closest match and has been experimentally found to produce the highest ionic conductivities of stabilized zirconia. However, yttrium, with an ionic radius of 104 pm, is the industry standard with a much more firmly established research base, lower costs, and better known long term stability.

1.2. Very Low Pressure Plasma Spray (VLPPS)

With very low pressure plasma spray, the plasma is formed in a chamber held at pressures around 100 to 600 Pa (0.75 to 4.50 Torr) [5]. Over this pressure range, the plasma jet expands to more than 20 cm in diameter and 1 m in length. In a study by Dorier et al, it was shown that plasma jet velocity and temperature increase with

decreasing pressure, while plasma jet density decreases [7]. In Table 1 below, a summary of these relationships can be seen.

Table 1. Measurements taken by Dorier et al 800 mm down the axis from the nozzle of a Sulzer Metco 03CP spray gun operated at 1500 A and 43 V, with plasma formed of H_2/Ar at 3/100 SLPM [7].

Pressure (Pa)	Plasma Velocity (m/s)	Plasma Temperature (K)	Plasma Density (kg/m^3)
200	3200	12500	0.75×10^{-4}
600	2500	11000	2.5×10^{-4}
1000	1000	7500	6.5×10^{-4}

Additionally, Dorier et al showed that, at 200 Pa, the velocity and temperature are virtually constant at radial distances up to 20 mm from the jet centerline. This was attributed to laminar flow of the plasma caused by limited interaction with the diffuse chamber atmosphere. In this environment, the mean free path of atoms in the plasma increases, leading to the likelihood that radiation increases in significance for heat transfer as the collision rate drops [6-12].

1.3. Suspension Plasma Spray (SPS)

Suspension plasma spray involves the use of a liquid medium and dispersants to suspend a powder feedstock that can then be injected into the plasma stream. By using suspensions, the minimum particle size is not limited by van der Waals interactions, as with dry powder feedstock. Suspensions also allow the addition of metal salts that decompose in the plasma and diffuse into the feedstock to enable composition control. Ethanol is the most common solvent used, due to its relatively low heat of vaporization, drawing 2.5 times less energy from the plasma than water based suspensions and resulting in almost a doubling of deposition efficiency [13,13,15]. A continuous laminar injection of suspension into the plasma core has been found to be the most effective method of injection. This produces a high velocity stream, with minimal variance, as the suspension penetrates into the plasma core and results in increased entrainment in the plasma [13,13].

2. EXPERIMENTAL PROCEDURE

The overall approach of this research was a parametric study of the combined VLPPS – SPS process, testing the effects of powder loading, gun power, gas composition, stand-off distance, dopant amount, and chamber pressure. Suspensions and substrates were prepared at Purdue University; then electrolyte coatings were applied at the TSRL. Finally, the coatings were analyzed at Purdue University using scanning electron microscopy (SEM), x-ray diffraction (XRD), surface profilometry, potentiodynamic testing, and impedance spectroscopy, as part of a complete fuel cell.

2.1. Suspension Preparation

Suspensions were prepared using 200 proof ethanol, 8 mole % YSZ powder, from Inframat Advanced Materials, and one of two dispersants. The particle size distribution of the YSZ powder can be seen in Figure 2, below.

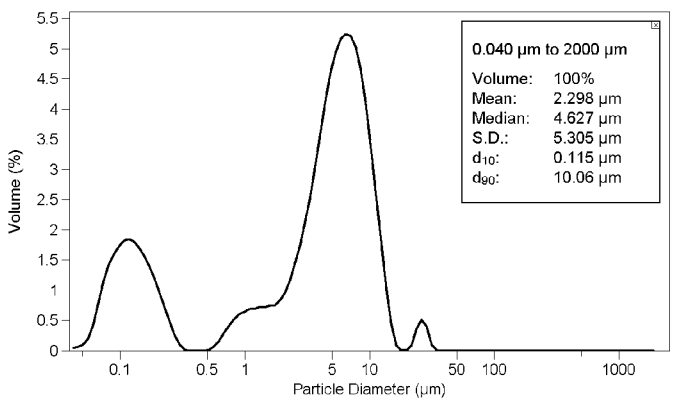

Figure 2. Coulter Counter measurement of particle size for 8 mole % YSZ from Inframat Advanced Materials.

The dispersants were either the phosphate ester Triton QS-44 or a low M_n (~1200) polyetheleneimine (PEI), both from Sigma Aldrich. Two different dispersants were necessary as the Triton QS-44 went out of production a year into research, although the use of PEI resulted in improved dispersion over Triton QS-44. Both dispersants were found to have optimal effectiveness at a weight fraction of 0.01. The amounts of each component were calculated based on equations 2, and 3, where V is volume (mL), ρ is density (g/mL), and w is weight fraction, with subscripts T, e, d, y, representing total, ethanol, dispersant, and YSZ, respectively.

$$\boldsymbol{V_T = V_e + V_d + V_y}$$

Equation 3

$$\frac{\boldsymbol{\rho_d V_d}}{\boldsymbol{\rho_e V_e + \rho_d V_d + \rho_y V_y}} = \boldsymbol{w_d}$$

Equation 4

In select suspensions, $Sc(NO_3)$-XH_2O, m_w 287.1 g/mol, was used as a doping agent. Dopants were added last, based solely on achieving the desired composition, as they were soluble in ethanol and did not play a role in powder dispersion. As such, the actual volume fraction of feedstock in doped suspensions was marginally lower than baseline suspensions. This small deviation was viewed acceptable as it allowed for batch production aimed at minimizing variation between suspensions. The final step of preparation was ball milling the suspensions for 3 hours in 500 mL baffled bottles. The suspensions were combined with 10mm YSZ cylindrical milling media and milled at ~140 rpm. An overview of suspension preparation can be seen in Figure 3, below.

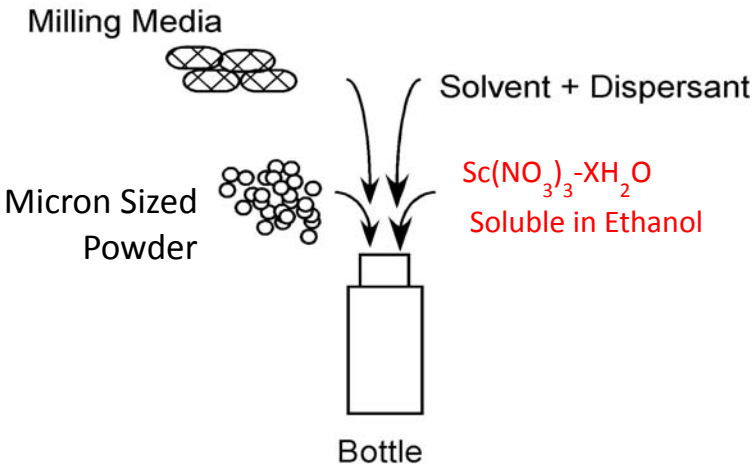

Figure 3. Overview of suspension preparation

2.2. Substrate Preparation

Substrates were designed to serve as the anode component of a SOFC. They were constructed out of 10 laminated sheets of tape cast NiO-YSZ, purchased from ESL Electroscience, with each layer a thickness of 180 µm. The sheets were laminated with a warm press and die, operated at 70 °C and 21 MPa, for 20 minutes. The resultant discs were then sintered at 1400 °C for 2 hours. The progression from tape casting to anode substrate can be seen in Figure 4, below.

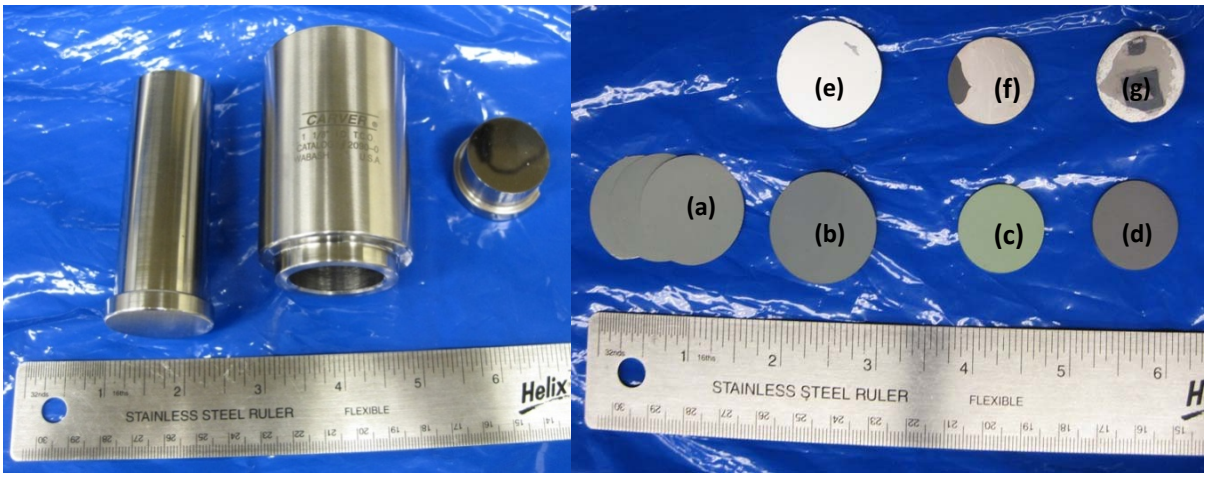

Figure 4. Images of the die (left) used to laminate the anode layers as seen on the right image showing the progression: (a) unlaminated sheets of NiO-YSZ, (b) hot-pressed laminated sheets of NiO-YSZ, (c) sintered laminated sheets of NiO-YSZ (in oxidized state), (d) sintered laminated sheets of NiO-YSZ (in reduced state), (e) an example of the initial material system used: NiO-YSZ with a YSZ electrolyte laminated sheet on top, (f) a sintered version of (e), in which the electrolyte delaminated, and (g) a complete fuel cell after testing, showing the cathode side (the white border is the bonding cement, the dark grey is the LSM-YSZ cathode material with platinum electrodes bonded to it, and the pearlescent area is exposed electrolyte)

2.3. Substrate Holders

Two types of substrate holders were used during the course of the research. The first was a stair step design allowing for simultaneous testing of three different stand-off distances, spaced 3” apart, as seen in **Figure 5**, below. This design was found to heat up rapidly during spraying, in excess of 1200 °C while the torch passed over it. It would then cool quickly enough, when the torch moved away, to cause the substrates to fracture. This required a reduction of plasma enthalpy in initial experiments via limiting gas composition and torch power.

Figure 5. Image of the stair step sample holder, with substrates loaded.

The second substrate holder was a water cooled copper plate, as seen in Figure 6, below. This substrate holder managed to reduce the heating of the substrates, enabling a wider range of plasma enthalpies to be tested, though it was insufficient to resolve the substrate cracking issue in the highest enthalpy range of the torch.

Figure 6. Image of the cold plate sample holder. This sample holder allowed for a reduction in substrate temperature and an increase in temperature stability over the course of a spray run.

2.4. Coating Creation at the Thermal Spray Research Laboratory

Electrolyte coatings were created in the TSRL's very low pressure plasma spray system, as shown in Figure 7, below, consisting of a ~3500 L water cooled vacuum chamber, a Sulzer Metco 03CA plasma torch, a 2000A, 50V Halmar power supply, and a suspension feed system. See Figure 8, below, for the dimensions of the cathode and anode setup.

Figure 7. Image of the vacuum chamber at the TSRL.

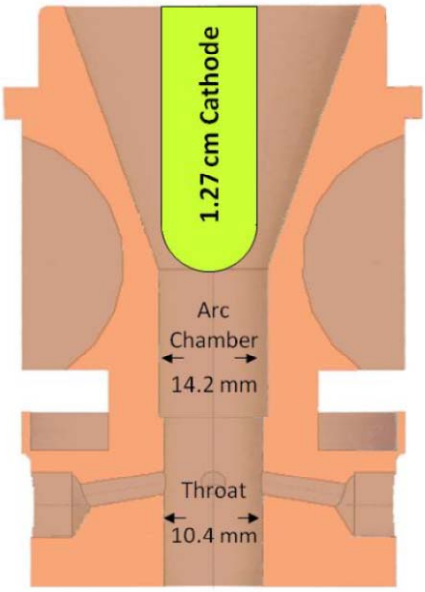

Figure 8. Diagram of the cathode and anode setup used at the TSRL.

All suspensions were injected orthogonally into the torch throat through a 230 µm diameter ruby straight hole nozzle, with a back pressure ~75psi, resulting in an injection velocity of ~20 m/s and a flow rate of ~43 g/min. Coatings were created during three visits in May 2010, summer 2011, and March 2012, here referred to as sample sets A, B, and C, respectively. The operating parameters of these visits can be seen in Table 2, Table 3, and Table 4, below.

Table 2. Operating parameters for samples created in May 2010 visit to TSRL.

A	**A1**	**A2**	**A3**	**A4**	**A5**
Feed (all QS-44)	0.5v%	0.25v%	1v%	3mSc	8mSc
Chamber Pressure (Torr)	2.4	2.4	2.4	2.4	2.4
Power	69	69	69	69	69
Gas Mix (Ar,H) (SLPM)	59, 7	59, 7	59, 7	59, 7	59, 7
Spray Time	7m	10m2s	10m	7m	7m

Table 3. Operating parameters for samples created in summer 2011 visit to TSRL.

B	**B1**	**B2**	**B3**	**B4**	**B5**	**B6**	**B7**
Feed (all PEI)	0.5v%	0.5v%	0.5v%	0.5v%	0.5v%	0.5v%	0.5v%
Chamber Pressure (Torr)	2.2	2.2	3.2	3.07	5.7	3.7	3.8
Amperage	1800	1800	1800	1800	1800	1200	1500
Voltage	49	49	49	44.5	49	45	45
Gas Mix (Ar, H, He) (SLPM)	60, 7, 56	60, 7, 56	60, 7, 56	60, 7, 56	60, 7, 56	60, 7, 56	60, 7, 56
Stand-off	35”	35”	36”	36”	36”	36”	36”
Spray Time	4m15s	5m	5m47s	3m1s	3m30s	7m13s	7m4s

Table 4. Operating parameters for samples created in March 2012 visit to TSRL.

C	C1	C2	C3	C4	C5
Feed (all 0.5v)	PEI	PEI	PEI	QS-44	QS-44
Chamber Pressure (Torr)	2.35	3.35	5.3	3.65	3.8
Amps	1500	1500	1500	1500	1600
Volts	38	40	42	40	42
Gas Mix (Ar,H,He) (SLPM)	59, 7, 19*	59, 7, 19*	59, 7, 19*	59, 7, 19*	59, 7, 19*
Stand-off	36”	35”	36”	36”	36”
Spray Time	8m 6s	15m 15s	8m 33s	8m 33s	8m 33s

Feed (all PEI)	1 v%	1v%	1v%	1v%	0.5v%	0.5v%
Chamber Pressure (Torr)	3.6	5.3	4.3	4.2	4	4.2
Amps	1500	1500	1500	1500	1500	1500
Volts	40	40.5	47	48	47	41
Gas Mix (Ar,H,He) (SLPM)	59, 7, 19*	59, 7, 19*	59, 7, 56	59, 7, 56	59, 7, 56	59, 7, 56
Stand-off	36”	36”	36”	36”	36”	36”
Spray Time	11m11s	8m33s	1-2m	8m33s	8m33s	5m

2.5. SOFC Testing at Purdue University

The samples brought back to Purdue, consisting of thin YSZ coatings on NiO-YSZ substrates, served as the basis for the creation of anode supported SOFCs. The substrates served as anode and the thin YSZ coatings as electrolytes, while a cathode material and electrodes were applied at Purdue using screen printing. A four point method was used in potentiodynamic testing and impedance spectroscopy, using a Solartron electrochemical interface SI 1287 and a Solartron impedance analyzer SI 1252. The layout of a fuel cell during testing can be seen in the diagram in Figure 9.

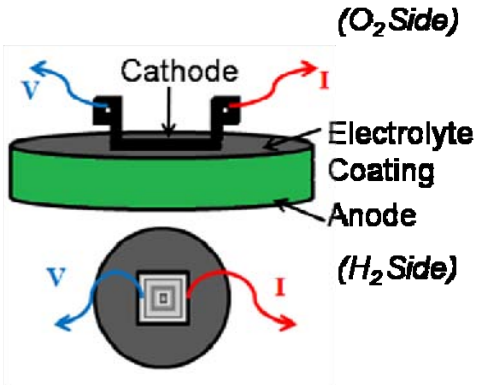

Figure 9. A diagram of a complete SOFC with electrodes attached using a four point method. A side view can be seen in the above image, while a top view/bottom view can be seen in the lower image.

An alumina paste served to seal the SOFCs to an alumina tube used to separate the H_2 rich anode from the exposed air (O_2 rich) cathode. This apparatus was then placed in a tube furnace and heated for testing at 800 – 1000 °C. An image of the testing rig can be seen in Figure 10, below.

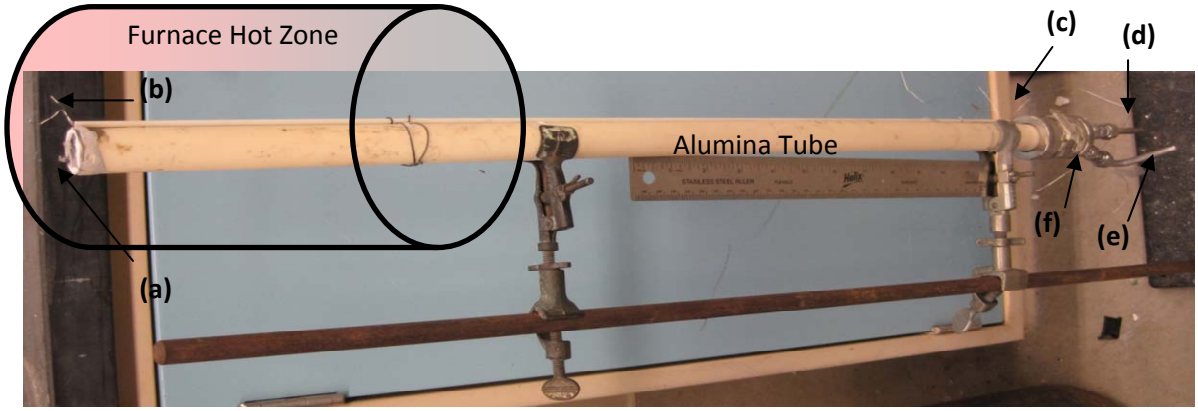

Figure 10. An image of the fuel cell testing rig outside of the furnace and fume hood, showing: (a) the cathode-side of the SOFC, (b) the cathode-side platinum electrode wires that attach to the fuel cell, (c) the cathode-side platinum wire measurement output connections, (d) the H2 gas input tube, (e) the exhaust gas tube (which feeds through two bubblers and out a fume hood), and (f) the anode-side platinum wire measurement output connections.

3. RESULTS & DISCUSSION

While understanding of this process has increased, reliability is an issue, associated, in part, with the complexity of the system. This research did serve to refine the suspension feed system at the TSRL enough to eliminate a former clogging issue in spray times up to 30 minutes. Fully adherent coatings were only achieved at pressures below 5 Torr and standoff distances greater than 36”, though these two factors were not fully isolated from each other by the time of this report. The maximum coating thickness was limited to ~10 µm before delamination from residual stresses occurred, with density of adherent coatings up to 90%. At the thicknesses and densities produced, these coatings were found to be too permeable for effective use as SOFC electrolytes.

Increased plasma enthalpy is a requirement brought on by suspension plasma spray in order to deposit fully molten feedstock. The full range of potential plasma enthalpy could not be tested due to the thermal shock sensitivity of the substrates used in this research. However, across the range of tested parameters, very similar microstructures were produced when coatings adhered to the substrates. While Helium addition did appear to increase plasma enthalpy, the increased overall gas flow rate itself increased the minimum maintainable chamber pressure by 1 Torr, as well as the size of the plasma jet, such that substrates would consistently fall in hotter regions of the plasma than in corresponding Helium free tests. As such, it is suggested that standoff distance should increase with increasing gas flow rate.

3.1. Scanning Electron Microscopy (SEM)

Scanning electron microscopy (SEM) was used as a basis for analysis of the effects of standoff distance, powder loading, spray time, and dopant concentration on the microstructure of SPS/VLPPS coatings. The as-sprayed microstructure can be seen in Figure 11, in which the presence of unmelted particles can be seen in the cross section as well as evidence of surface roughness in both micrographs. Figure 12 shows the microstructure of a complete fuel cell after testing, which includes a 2 hour heat treatment at 1200º C. This heat treatment causes some sintering of the electrolyte, though the density is still around 90%.

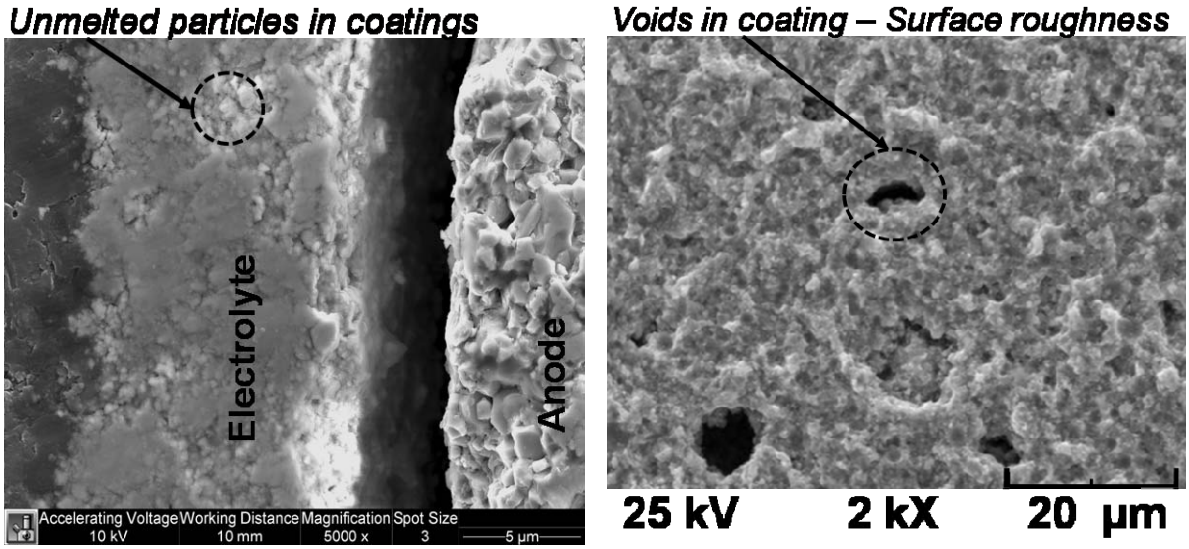

Figure 11: SEM images of the initial microstructures of select SPS/VLPPS coatings. On left is a cross-section of an un-doped 1 vol.% YSZ coating sprayed for 10 minutes at 46" standoff. On right is a surface image of a 3 mol% Sc-doped 0.5 vol.% YSZ coating sprayed for 7 minutes at 43". Note the presence of unmelted particles in the cross-section image, despite significant density of the coating, and the surface roughness of the right image.

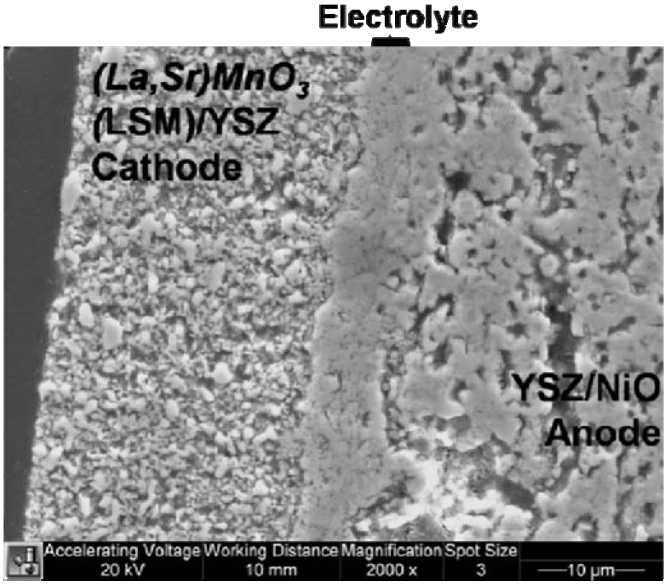

Figure 12: SEM image of a complete fuel cell after testing. The spray conditions were 8 mol% Sc-doped 0.5 vol% YSZ, sprayed for 7 min at 49". Note that in the fuel cell preparation, the coating undergoes a 1200º C - 2 hour heat treatment, which causes some sintering and the subsequent disappearance of clear remnant particles in the coating, as seen in Figure 11.

The effect of standoff distance on electrolyte coating thickness was shown to be negligible within the tested range 43"-49", while surface roughness of the coating can be seen as the ultimate limiting factor on the minimum achievable coating thickness.

Due to the thin geometries of these coatings, the effect of a few microns of surface roughness did serve to obfuscate the standoff distance findings somewhat. In Figure 13, a comparison of undoped electrolyte coatings can be seen. In Figure 14 and Figure 15, a comparison of 8 mol. % Sc doped coatings can be seen at different magnifications. In comparing all 3 sets of images, no distinct difference in thickness can be attributed to stand-off distance.

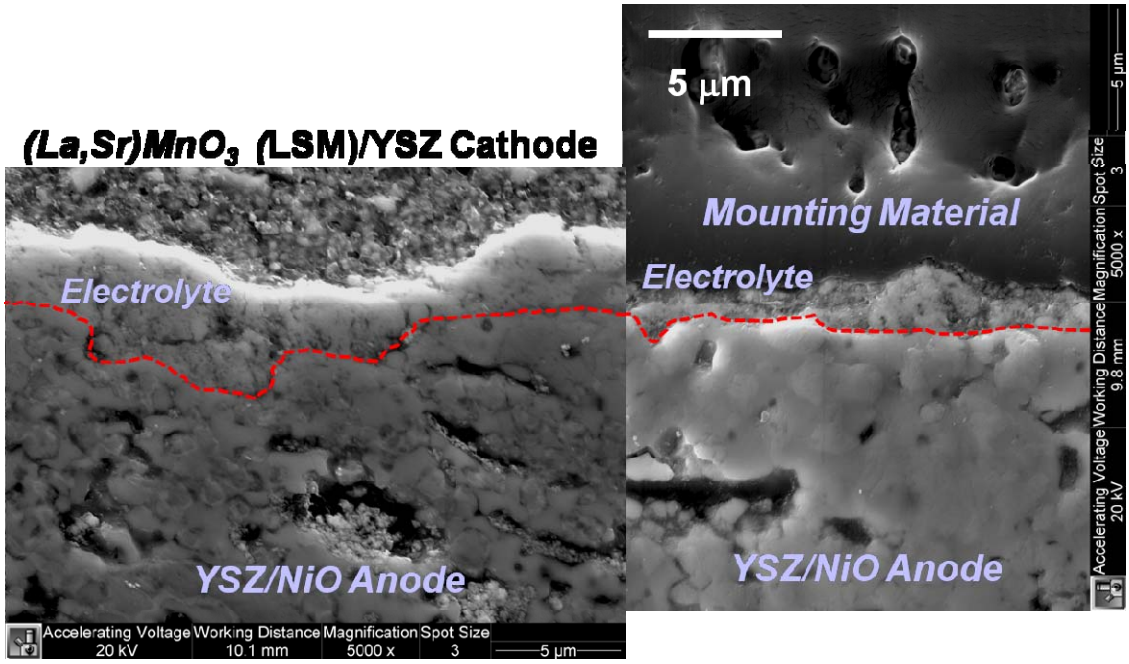

Figure 13: SEM images of 0.5 vol% YSZ, sprayed for 7 min at 43" (left) and 49" (right). While this comparison would suggest a moderate increase in thickness for the closer standoff distance, this is attributed to the surface roughness induced variability in coating thickness associated with comparing any two individual sections of coatings. See Figure 14 and Figure 15 for further evidence of this.

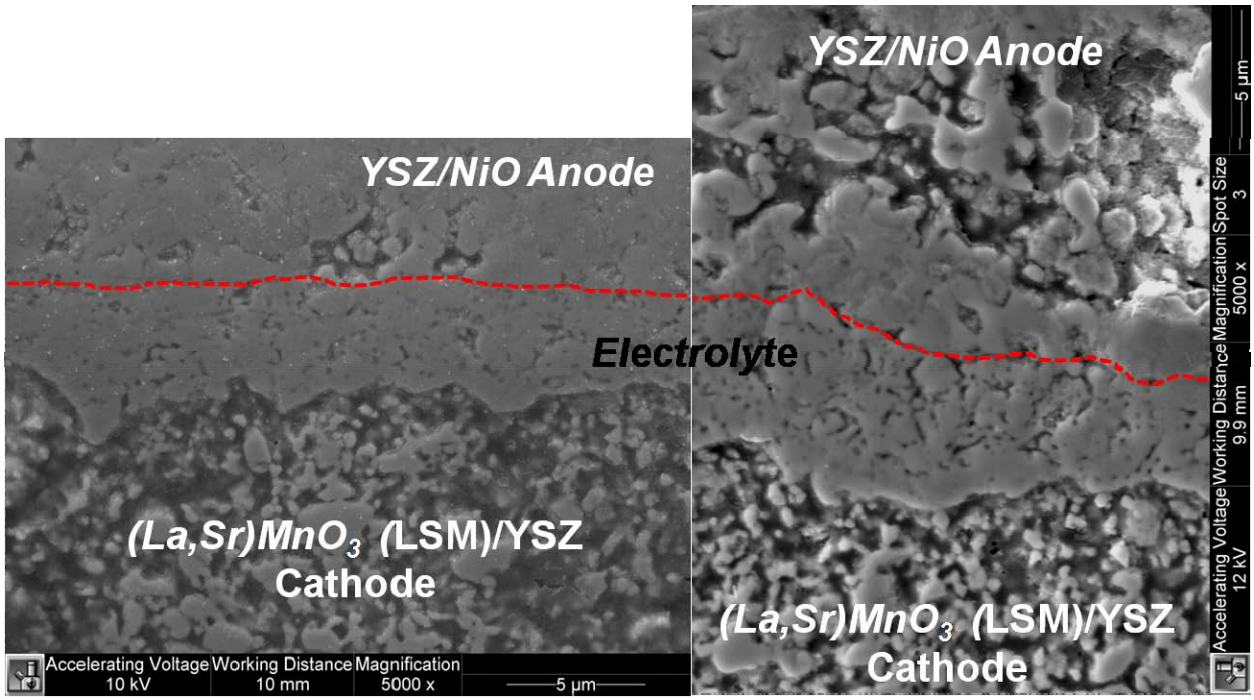

Figure 14: SEM images of 8 mol. % Sc-doped 0.5 vol% YSZ, sprayed for 7 min at 43" (left) and 49" (right). This comparison suggests a slight increase in coating thickness caused by increasing standoff distance within this 6" range. However, as seen in Figure 13, this is a byproduct of the bias associated with comparing any two small sections of coatings. See Figure 15 for further evidence of this.

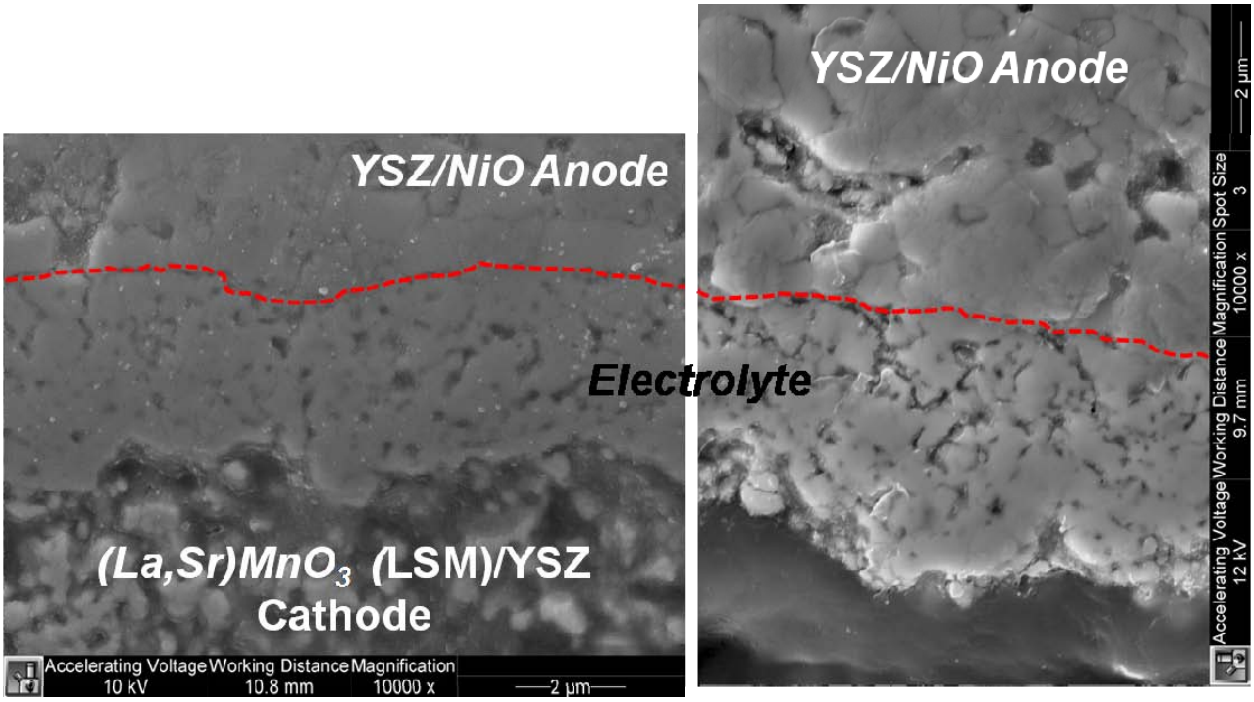

Figure 15: SEM images at higher magnification of the same coatings from Figure 14, 8 mol. % Sc-doped 0.5 vol% YSZ, sprayed for 7 min at 43" (left) and 49" (right). This comparison suggests there is no effect on coating thickness caused by changing standoff distance within this 6" range. See Figure 13 and Figure 14 for further evidence of this.

The effect of powder loading on electrolyte coating thickness showed a clear trend that can be approximated as ~(1.1 µm/min)*vol.%. The surface roughness was shown to increase somewhat with increasing thickness, the extreme of which was only achieved at the highest powder loading, so this effect cannot yet be isolated from powder loading. However, the surface roughness relative to overall coating thickness actually went down as coating thickness increased. A comparison between 0.25 vol.% and 1 vol.% powder loading, showing the increased coating thickness with increased powder loading, can be seen in Figure 16.

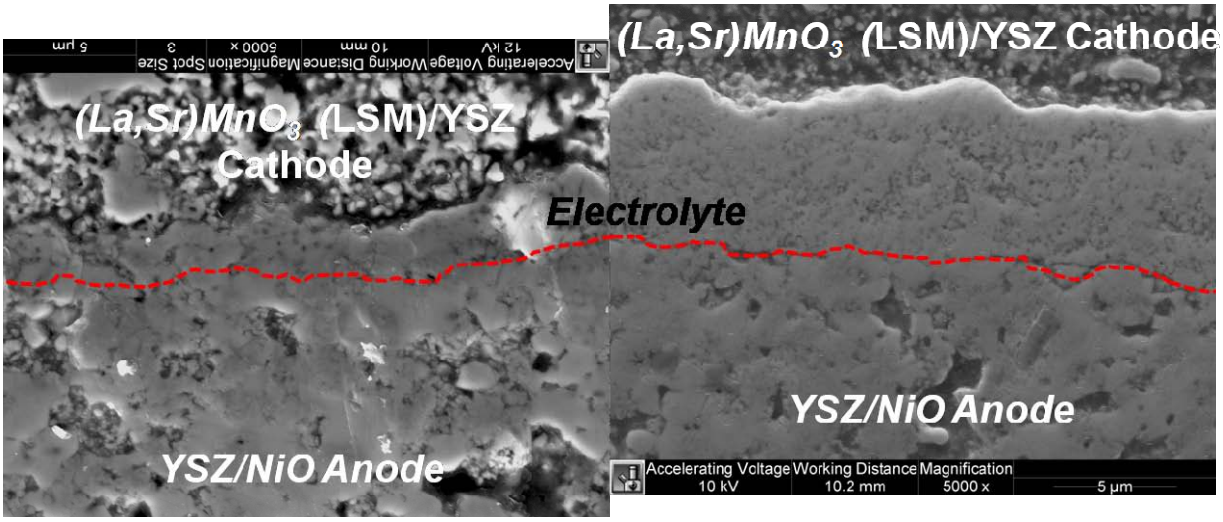

Figure 16: SEM images of 0.25 vol.% YSZ (left) and 1 vol.% YSZ (right), sprayed for 10 min at 43" (left) and 49" (right). As expected, this comparison shows a distinct increase in coating thickness associated with increased powder loading.

The microstructure of the 3 mol.% Sc and 8 mol.% Sc doped electrolyte coatings was found to be very similar and to be relatively indistinguishable from the undoped coatings, as seen in Figure 17. The true distinguisher of doping was found in the EDS spectrum, as evidenced in the EDS map seen in Figure 18. As such, it is believed that the dopant is in solid solution with the YSZ. It is important to note that the suspension doping does not equal the doping of the resultant coating. Previous doped SPS research has shown a ~50% doping rate. Also, since the net dopant molecule formed is Sc_2O_3, the net doping of the coating is halved. For example, when a suspension is doped with 8 mol. % Sc, the likely net doping of the coating is around 2 mol.% Sc_2O_3. XRD analysis of these coatings can be seen in Figure 19, in which no evidence of a Sc_2O_3 phase can be seen.

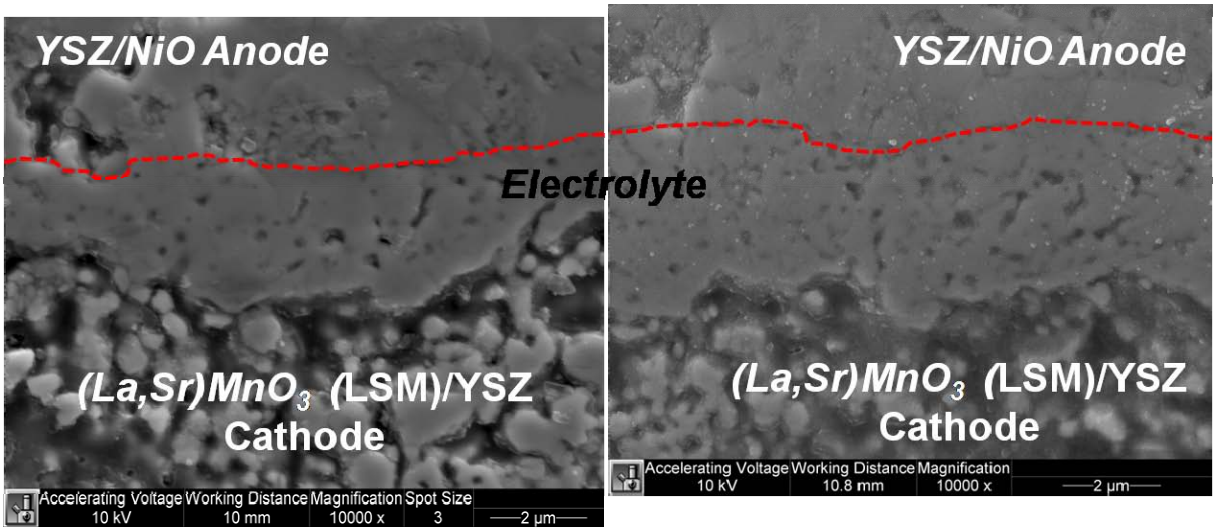

Figure 17: SEM images of 0.5 vol% YSZ, sprayed for 7 min at 43" with doping of 3 mol% Sc (left) and 8 mol% Sc (right). The microstructures are too similar to mark a definitive difference between the doping levels, though initial fuel cell testing has shown increasing performance with doping.

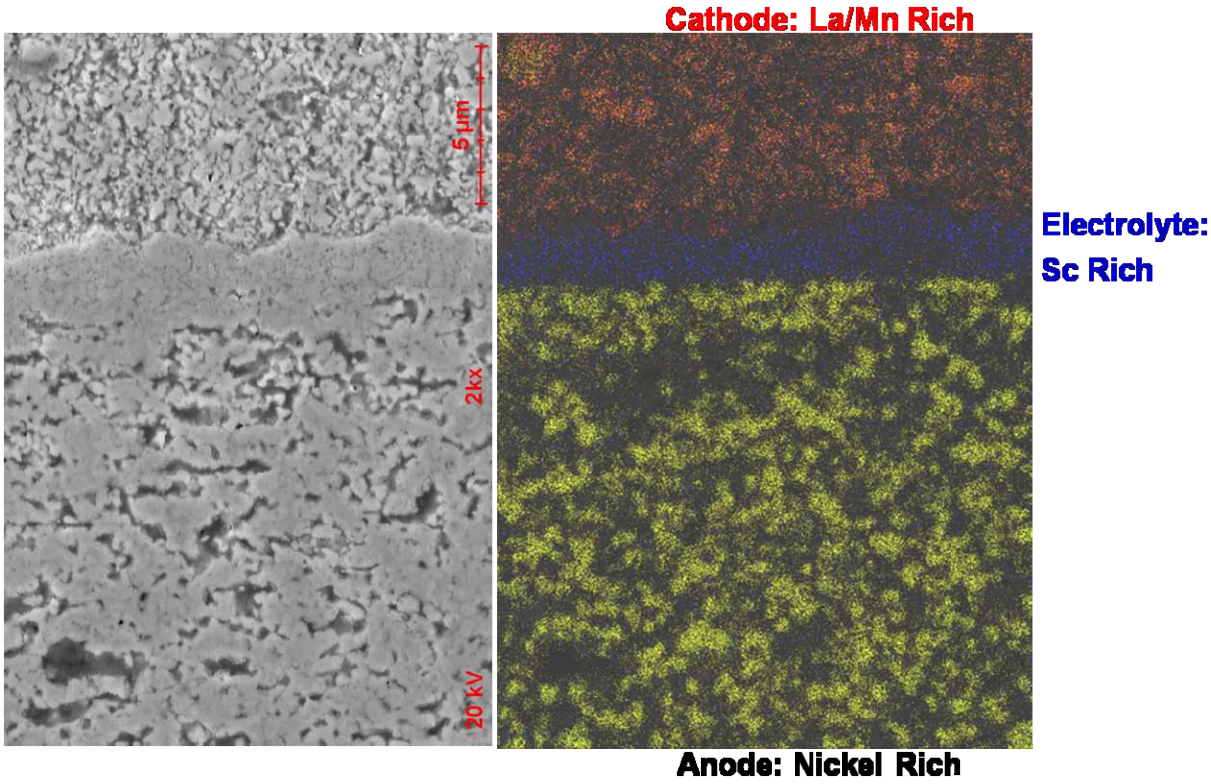

Figure 18: SEM image and EDS map of a complete fuel cell with an electrolyte created with 8 mol% Sc-doped 0.5 vol% YSZ, sprayed for 7 min at 49". The EDS map clearly shows the presence of scandium (blue) in the electrolyte.

3.2. X-Ray Diffraction (XRD)

The XRD analysis, in conjunction with EDS measurement of scandium content in doped coatings, supports the supposition that scandium diffuses into the zirconia lattice during SPS/VLPPS. As seen in Figure 19, below, no Scandia associated peaks are present in the doped samples. The peaks did shift left slightly in the doped samples, as might be expected with the presence of the smaller Sc (in comparison to Y) in solid solution, though this was viewed to be within the error of measurement for these samples, due to the imperfect plane formed by the substrate.

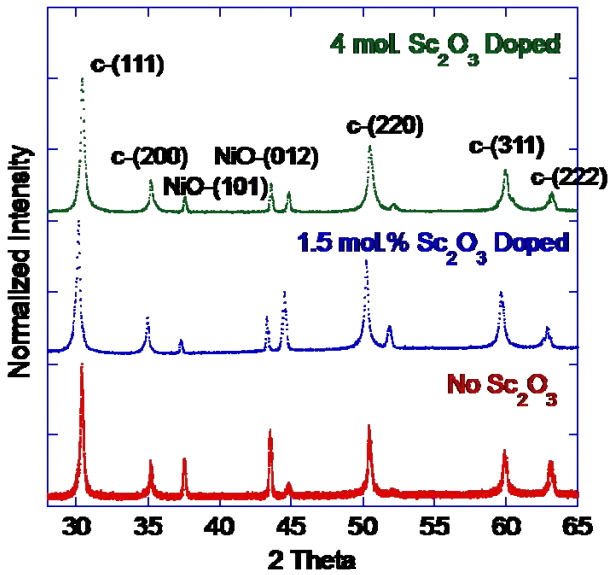

Figure 19: XRD spectrum comparison between undoped, 1.5 mol% Sc_2O_3, and 4 mol% Sc_2O_3 electrolyte coatings prepared on a NiO-YSZ substrate. No peaks were associated with a separate Sc_2O_3 phase.

3.3. Fuel Cell Performance

The fuel cell testing of the electrolyte coatings has shown improvement with Sc doping, however an initial flaw in the testing resulted in low current densities, negating the impact of these results. Standard fuel cells were purchased from Fuel Cell Materials, Inc in an effort to compare results given this limitation and as a method to clarify the testing flaw. This lead to an improvement in the testing procedure, though the coatings tested at that point were created using different process parameters from the initial testing that proved to produce coatings of insufficient quality for fuel cell testing.

However, with the improvement of the testing procedure came validation of the open circuit voltage (OCV) measurements of all tests. This consistently showed the SOFCs produced from SPS/VLPPS electrolytes to be of low quality. In Figure 20, the results are shown of the performance comparison of the standard cell and the best SPS/VLPPS fuel cell produced, when tested using the initial low current density method. The power

density performance is comparable, though again, an important point to note is the more accurately measured OCV, which is the y-axis intersection of the IV curve, representing the electromotive force of the reaction, which should be around 1.1V, as the standard cell is.

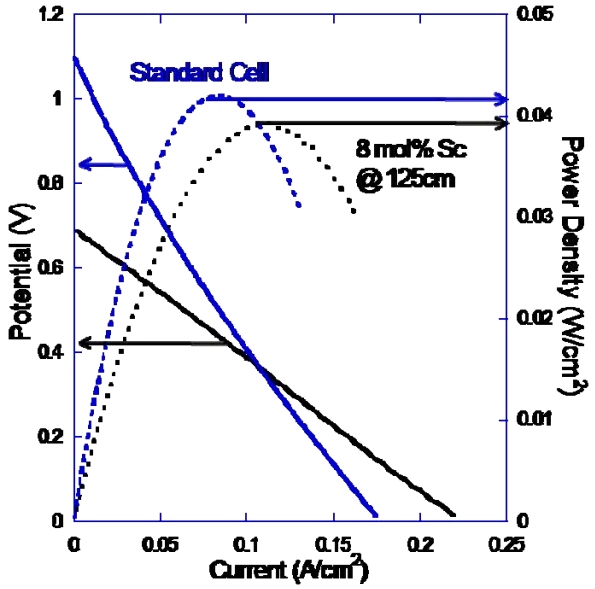

Figure 20: Potentiodynamic testing results comparing an 8 mol% Sc doped 0.5 vol% YSZ, sprayed for 7 min at 49" to a standard cell, made from similar components, including a YSZ electrolyte, purchased from Fuel Cell Materials, Inc.

The OCV of SPS/VLPPS electrolyte SOFCs was found to be dependent on the electrolyte thickness, with the thickest coating, ~11 µm, having 0.93V. This thickness relationship is attributed to porosity in the coating allowing for a leakage current at lower thicknesses. However, experiments in which thicker coatings were attempted resulted in delamination.

4. CONCLUSIONS

This project advanced Sandia's capability in the area of very low pressure plasma spray (VLPPS) and suspensions plasma spray (SPS). This coating technology is still emerging with the capability to prepare coatings in thickness/density regimes not currently accessible with conventional thermal spray or thin film processes. Improved ability to effectively prepare dense coatings in the 1 – 100 micron thickness regime with a wide range of compositions also allows for new coating solutions to be realized for broad based application across DOE mission space including work associated with NW, Energy, and National Security missions, as well as support of Other Federal Agencies.

By combining SPS with VLPPS, thin and dense electrolytes of appropriate composition for SOFCs are possible. By working at pressures as low as 2.4 Torr, energy partitioning in the plasma and its interaction with the surrounding chamber atmosphere is dramatically reduced. The result is a significant increase in plasma mean free path length and plasma velocity. This causes the plasma to remain coherent longer and deposit uniformly over larger areas. It also increases the total time particles are entrained in the plasma and consequently the amount of energy these particles absorb.[2] The increased residence time in the plasma resulted in Scandium dopant atoms being incorporated into the coating. Interestingly, no Scandium Oxide peaks were present in XRD of the coating, indicating that Scandium Oxide is not present in the finished coating. Chemical analysis (EDS), however, confirmed the presence of Scandium in the coating. This suggests that Scandium atoms have been incorporated into the Zr_2O_3 coating material.

These data and data from others show that compounds dissolved in the suspension (i.e. dopants) are incorporated into the coating during plasma spraying.[3] Thus, it is possible to change the chemistry of the coating material during the short (milliseconds) time the powder/dopant mixture is in the hot spray plume. This means that it is possible to quickly and systematically change the composition of the sprayed SOFC electrolyte to optimize its oxygen-ion conductivity by simply adjusting the suspension composition. It also means that that an entire fuel cell could be created with this single piece of equipment, using both composition and porosity graded coatings to create each component in sequence. This coating control capability has the potential to significantly improve the state of the art in SOFC production, but requires further research to reach that point.

---

[2] Spinhirne, N., *The Development and Characterization of Novel Yttria-Stabilized Zirconia Coatings Deposited By Very Low Pressure Plasma Spray*, New Mexico Institute of Mining and Technology, 2008 p. 13-46.
[3] Every, Kent, *Development and Evaluation of Suspension Plasma Sprayed Yttria Stabilized Zirconia Coatings as Thermal Barriers*, Purdue University, 2009, p. 41.

4.1. List of Publications, Presentations, Awards, etc.

A paper reviewing the VLPPS process was co-written with lead author Mark Smith and published in Coatings **2011**, *1*, 117-132, titled Very Low Pressure Plasma Spray—A Review of an Emerging Technology in the Thermal Spray Community [5].

Results have been presented at the MS&T 2010, MS&T 2011, and ITSC 2011 conferences. A presentation will also be given at the MS&T 2012 conference. Article submissions to high quality peer reviewed scientific journals will occur as the research progresses.

5. REFERENCES

1. Singh, P; Minh, N, *Solid oxide fuel Cells: technology status*, International Journal of Applied Ceramics Technology, 1, 2004, pp. 5-15.
2. U.S. Department of Energy. *FCT Fuel Cells: Types of Fuel Cells.* 2009. Retrieved from http://www1.eere.energy.gov/hydrogenandfuelcells/fuelcells/fc_types.html
3. Guo, X, *Can We Achieve Significantly Higher Ionic Conductivity in Nanostructured Zirconia?*, Scripta Materialia, 65(2), July 2011, pp. 96-101.
4. Li, P. and Chen, I., *Effect of Dopants on Zirconia Stabilization-An X-ray Absorption Study: I, Trivalent Dopants*, J. Am. Ceram. Soc., 77(1), 1994, pp. 118-128.
5. Smith, M; Hall, A.; Fleetwood, J.; Meyer, P. *Very Low Pressure Plasma Spray - A Review of an Emerging Technology in the Thermal Spray Community*, Coatings, 1, 2011, pp. 117-132.
6. Spinhirne, N., *The Development and Characterization of Novel Yttria-Stabilized Zirconia Coatings Deposited By Very Low Pressure Plasma Spray*, Masters Thesis, New Mexico Institute of Mining and Technology, 2008, pp. 13-46.
7. Dorier, J.; Gindrat, M.; Hollenstein, Ch.; Loch, M.; Refke, A.; Barbezat, G. *Plasma jet properties in a new spraying process at low pressure for large area thin film deposition*, In Proceedings of the 2001 International Thermal Spray Conference, Singapore, 28–30 May 2001, pp. 1-6.
8. Jodoin, B.; Gindrat, M.; Dorier, J.L.; Hollenstein, C.; Lcoh, M.; Barbezat, G. *Modeling and diagnostics of a supersonic DC plasma jet expanding at low pressure*. In Proceedings of the International Thermal Spray Conference, Essen, Germany, March 2002, pp. 716-720.
9. Gindrat, M.; Dorier, J.-L; Hollenstein, Ch.; Loch, M.; Refke, A.; Salito, A.; Barbezat, G. *Effect of specific operation conditions on the properties of LPPS plasma jets expanding at low pressure*. In Proceedings of the International Thermal Spray Conference, Essen, Germany, March 2002, pp. 459-464.
10. Bolot, R.; Klein, D.; Coddet, C. *Design of a nozzle extension for thermal spray under very low pressure conditions*. In Proceedings of the International Thermal Spray Conference, Osaka, Japan, May 2004, pp. 574-579.
11. Kingswell, R.; Scott, K.T.; Wassel, L.L. *Optimizing the vacuum plasma spray deposition of metal, ceramic, and cermet coatings using designed experiments*. J. Therm. Spray Technol. 1993, *2*, pp. 179-185.
12. Bolot, R.; Sokolov, D.; Klein, D.; Coddet, C. *Nozzle developments for thermal spray at very low pressure*. J. Therm. Spray Technol. 2006, *15*, pp. 827-833.
13. VanEvery, K., *Development and Evaluation of Suspension Plasma Sprayed Yttria Stabilized Zirconia Coatings as Thermal Barriers*, Doctoral Thesis, Purdue University, 2009.
14. Siegert, R., *A Novel Process for the Liquid Feedstock Plasma Spray of Ceramic Coatings with Nanostructural Features*, Doctoral Thesis, Institut fur Werkstoffe und Verfahren der Energietechnik, 2005.

15. Chen, Z., Trice, R., *Air-plasma spraying colloidal solutions of nanosized ceramic powders*, Journal of Materials Science, 39, 2004, pp 4171-78.

DISTRIBUTION

1 Dr. Rodney Trice (electronic copy)
701 Stadium Avenue
West Lafayette, IN 47907

1 Mr. James Fleetwood (electronic copy)
701 Stadium Avenue
West Lafayette, IN 47907

1 Dr. Elliott Slamovich (electronic copy)
701 Stadium Avenue
West Lafayette, IN 47907

1	MS1130	Aaron Hall	01832 (electronic copy)
1	MS1130	James Mccloskey	01832 (electronic copy)
1	MS0889	Deidre Hirschfeld	01832 (electronic copy)
1	MS0899	Technical Library	9536 (electronic copy)
1	MS0359	D. Chavez, LDRD Office	1911 (electronic copy)

Sandia National Laboratories